AE 460 Laboratory Note for Experiment 1

Wind Tunnel Calibration

by

Prahersh Kumar, Shyam Murali Thyagarajan, Blizhaid Alexis Estrada Reyes, Dylan D'Silva,

TA: Jack Mills

Section ABT, Group A, Wednesday, 7:00-9:00 pm

Submitted on 9/14/2022

1 INTRODUCTION

This lab was an introduction to wind tunnel operation and data acquisition. The goal of the lab was to use pressure and temperature data readings to determine multiple flow characteristics across the test section of an open circuit, low speed wind tunnel for multiple motor rotation rates. Multiple static and total pressure measurements within the wind tunnel test section were taken using a pressure rake in the test section for incremented motor rotation rates ranging from 400 to 1400 rotations per minute. The dynamic pressure was then found using the static and total pressure measurements and used to calculate the speed of the flow across the test section. With the airspeed known, Mach and Reynolds numbers were calculated, as well as the variation total and dynamic pressure across the test section. These served as an introduction to operating the wind tunnel, using LabView to acquire and store data from the wind tunnel measurements, and perform analyses with the data.

2 APPARATUS

The experiment was conducted using an Aerolab Low-Speed Wind Tunnel with a static pressure ring connected to the outside of the wind tunnel. The static pressure ring collected the static pressure on the four outside walls of the wind tunnel, representing the average total pressure outside the wind tunnel. A Dwyer Model 246 inclined manometer was used to measure the difference between the atmospheric pressure and the static pressure as measured by the static pressure ring. The difference in pressure represents a corrective term for the static pressure ring measurement to find absolute pressure. The difference in pressure is also obtained from an Omega PX653 Pressure Transmitter, but this pressure transmitter collects the data in LabView. The differential values acquired with this pressure transducer were collected by the LabView software on the connected computer. Within the test section of the wind tunnel, a rake lay on the section's lateral centerline. The rake consisted of 13 pressure probes on 4 arms which collected static and total pressure data. Each of the four arms had two total pressure probes and one static pressure probe. A pitot-static probe was located

in the center of the four arms. A PSI NetScanner model 9016 pressure transducer was used to record the pressure measurements from the rake relative to the static pressure ring measurements. LabView code processed the pressure data acquired by the PSI NetScanner and transferred the data to the computer connected to the PSI NetScanner system. A Control Company Model 4195 compact digital manometer was used to measure atmospheric pressure and temperature within the laboratory. The following table shows each major component used in the experiment, as well as its measurement uncertainty and what it was used for.

Table 1: Apparatus Components

Component Identification	Measurement Uncertainty	Use
Aerolab Low-Speed Wind Tunnel	N/A	Provide airflow for testing
Static Pressure Ring	N/A	Determine total pressure
Dwyer Model 246 Inclined Manometer	1% of full scale	Measure Atmospheric Pressure Difference
Omega PX653 Pressure Transmitter	0.25% of full scale	Measure atmospheric pressure difference in LabView
Static and Total Pressure Probes	N/A	Measure test section airflow static or total pressure
PSI NetScanner Model 9016	0.1% of full scale	Record rake pressure probe data
Control Company Model 4195 Pressure Transducer	0.148" Hg and 1.8°F	Measure atmospheric pressure and temperature

The figure below is a schematic of the basic set-up of the wind tunnel for this experiment.

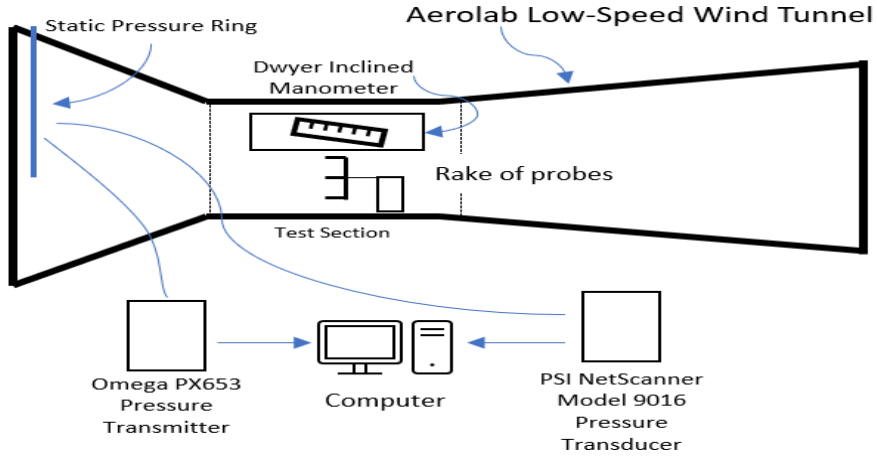

Figure 1: Schematic of wind tunnel pressure measurement system for determining dynamic pressure

The following figure illustrates the layout of the pressure probe rake that is present in the wind tunnel:

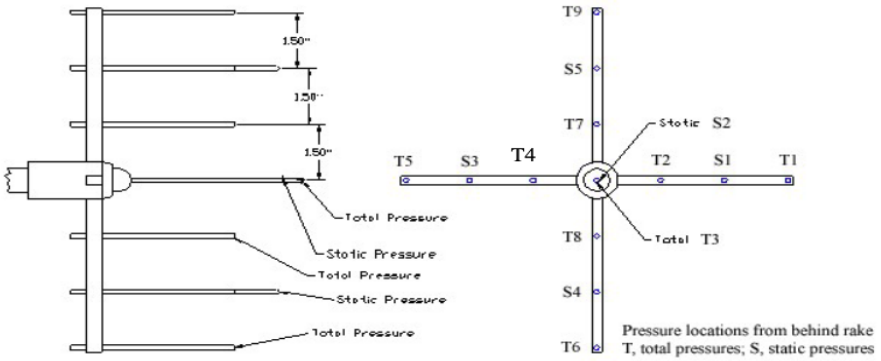

Figure 2: Schematic of Pressure Probe Rake

3 RESULTS AND DISCUSSION

3.1 Actual/Average Dynamic Pressure Calculations

Table 2: Average Dynamic Pressure

Data Point	Motor Speed [rpm]	P_{0avg} [psid]	P_{Savg} [psid]	q_{actual} [psid]
1	400	4.72E-03	5.24E-05	4.67E-03
2	500	7.82E-03	8.68E-05	7.73E-03
3	600	1.16E-02	2.06E-04	1.14E-02
4	700	1.65E-02	2.48E-04	1.62E-02
5	800	2.20E-02	2.28E-04	2.18E-02
6	900	2.79E-02	5.65E-04	2.73E-02
7	1000	3.47E-02	6.87E-04	3.40E-02
8	1100	4.30E-02	6.66E-04	4.24E-02
9	1200	5.23E-02	3.99E-04	5.19E-02
10	1300	6.07E-02	7.04E-04	6.00E-02
11	1400	7.07E-02	1.26E-04	7.06E-02

Table 2 outlines the changes in the average total pressure (P_{0avg}), the average static pressure (P_{Savg}), and the dynamic pressure (q_{actual}) over the range on motor speeds that we tested. The values for the average total pressure (P_{0avg}) and the average static pressure (P_{Savg}) were calculated

by averaging the measurements from the individual total pressure probes and static pressure probes respectively at each motor speed:

$$P_{0avg} = \frac{\sum P_{0i}}{i} \text{ and } P_{Savg} = \frac{\sum P_{Si}}{i} \tag{1}$$

In the equation above P_{0i} and P_{Si} represent the total or static pressure from one of the nine total pressure probes or one of the five static pressure probes. From this we found the dynamic pressure (q_{actual}) at each motor speed by using the following equation:

$$q_{actual} = P_{0avg} - P_{Savg} \tag{2}$$

Observing the table we see the general trend of P_{0avg}, P_{Savg}, and q_{actual} increasing as the motor speed increases. This is expected as we are forcing a larger volume of air to move through the same sized section as we increase the motor speed.

3.2 Velocity, Reynolds Number, and Mach Number at Various Motor Speeds

Before we can find the velocity, Reynolds number, or mach number we first have to find the density of the air in the test section. To do this we will utilize the following equation where R represents the gas constant of air (sample calculations are located in the appendix):

$$\rho = \frac{p_{ambient}}{R * T_{ambient}} = 0.00225 \frac{lb}{ft^3} \tag{3}$$

Once we found the density we are then able to solve the the actual velocity (V_{actual}) of the air inside the test section at each given motor speed. To do this we use the following equation (sample calculations are located in the appendix):

$$V_{actual} = \frac{2 * q_{actual} * 144}{\rho} \tag{4}$$

Now that we have the V_{actual} we can calculate the Reynolds Number per unit length and Mach

number for each motor speed using the following two equation (sample calculations are located in the appendix):

$$\frac{Re}{L} = \frac{\rho * V_{actual}}{\mu} \tag{5}$$

$$M = \frac{V_{actual}}{\sqrt{\gamma * R * T_{ambient}}} \tag{6}$$

The value for γ (ratio of specific heats) is 1.4. μ is the viscosity of the gas in the test section. Once we calculated the values for V_{actual}, the Reynolds Number, and the Mach number for each data point we compiled out results into the following table (Table 3).

Table 3: Motor Speed effect on Test Section values

Data Point	Motor RPM	q_{actual}[psid]	V_{actual}[ft/s]	Reynolds Number 1/ft	Mach Number
1	400	4.67E-03	24.42	144153.74	0.022
2	500	7.73E-03	31.43	185556.83	0.028
3	600	1.14E-02	38.18	225419.85	0.034
4	700	1.62E-02	45.53	268823.91	0.040
5	800	2.18E-02	52.76	311525.34	0.047
6	900	2.73E-02	59.11	348989.57	0.052
7	1000	3.40E-02	65.89	389022.54	0.058
8	1100	4.24E-02	73.57	434364.18	0.065
9	1200	5.19E-02	81.44	480858.77	0.072
10	1300	6.00E-02	87.56	516978.72	0.077
11	1400	7.06E-02	94.98	560755.45	0.084

We then graphed the values of q_{actual}, V_{actual}, Reynolds Number, and Mach Number against Motor Speed to get the following graphs:

Figure 3: Top Left: Actual Dynamic Pressure vs Motor Speed, Top Right: Actual Velocity vs Motor Speed, Bottom Left: Reynolds Number vs Motor Speed, Bottom Right: Mach Number vs Motor Speed

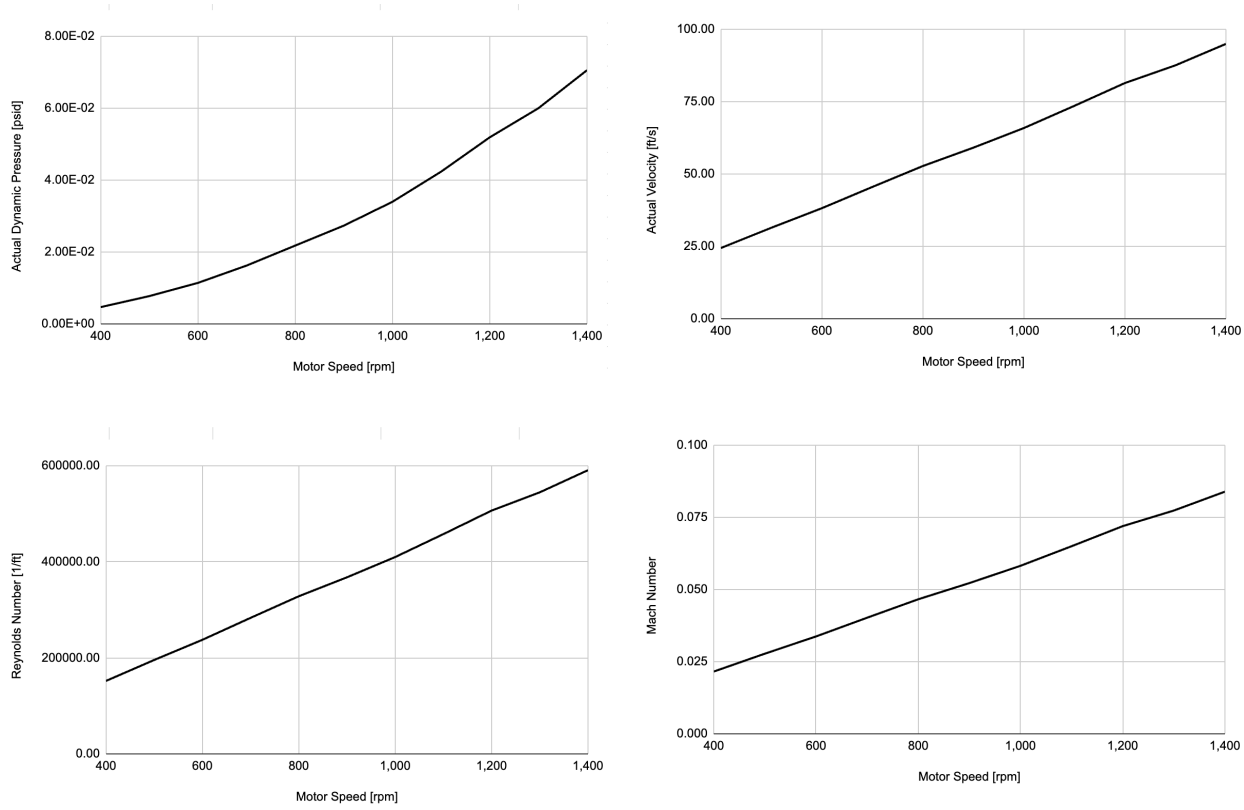

From the equations used to calculate the V_{actual} we would expect $V_{actual}^2 \propto q_{actual}$. We see that this is true as the graph for q_{actual} appears to increase in an exponential fashion and the graph for the V_{actual} appears to increase in a linear fashion. Additionally the graphs for the Reynolds and Mach number also appear to increase in the expected pattern as they should be proportional to V_{actual} graph which they are.

While these graphs are useful for estimating the expected properties inside of a wind tunnel when we conduct future experiments they will only provide us with rough estimates as the ambient conditions inside and around the wind tunnel may be different. These changes will in turn effect the value of the air density leading to these graphs only providing us with approximate values for a given property at a given Motor Speed.

3.3 Variation of the Total and Dynamic pressures across the Wind Tunnel

In order to compare the variation in the total and dynamic pressure from the different probes on the rake, calculate the percent difference of each total/dynamic pressure from the average total/dynamic pressure, normalizing the difference by the average dynamic pressure. We firstly calculated the variation of the total pressure (TPV_i) at each motor speed by using the following equation:

$$TPV_i = \frac{P_{0i} - P_{0avg}}{q_{actual}} * 100[\%] \tag{7}$$

After doing this for every total pressure probe at each data point and plotting we get the following graph:

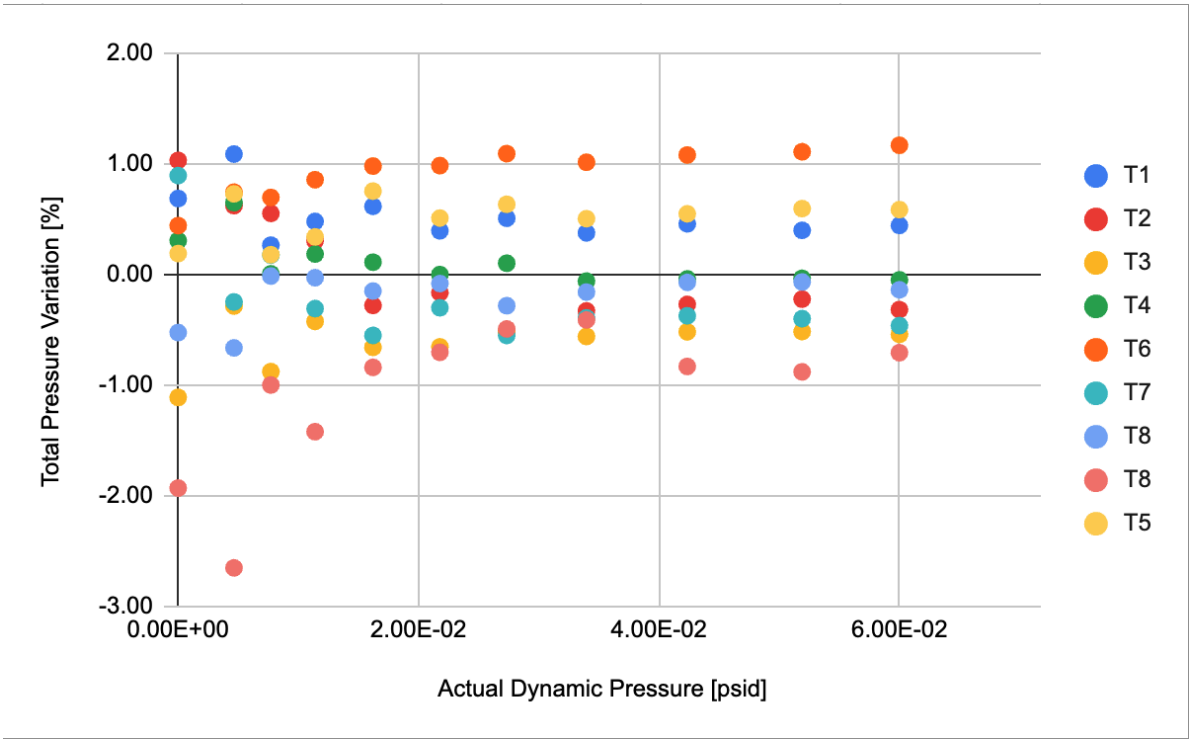

Figure 4: Total Pressure Variation TPV_i [%] vs Actual Dynamic Pressure [psid]

To find the static pressure variation we followed a similar process:

$$SPV_i = \frac{P_{Si} - P_{Savg}}{q_{actual}} * 100[\%] \tag{8}$$

Plotting the results we got (Note the second to last pink dot should be labeled T9):

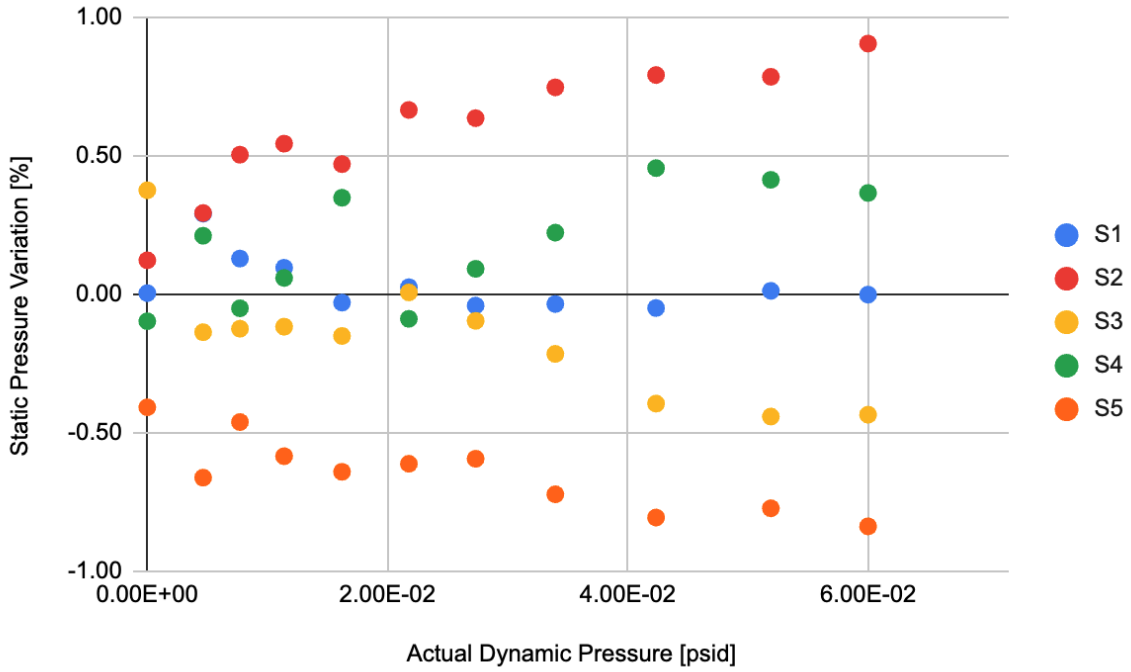

Figure 5: Static Pressure Variation TPV_i [%] vs Actual Dynamic Pressure [psid]

We notice some interesting patterns in both the Figure4 and in Figure5. In Figure4 we notice that the total pressure readings appear to have a greater variation than the static pressure readings that are presented in Figure5. All the static pressure probes appear to be within 1% of the average while the total pressure readings vary up to 2% with many of the readings being clustered around ±1%. This may be due to the fact that the distribution of total pressure probes are further apart or due to a boundary layer being formed at the tip of the probe changing the pressure before the total pressure can be read by the sensor.

Another interesting pattern we see in Figure4 is that the probes closer to the center of the pressure rake appear to have the least variation from the average. A noticeable exception is T3 which is the center probe which appears to stray further away from the average than probes T2, T4, T7, and T8. In Figure5 S2, which is the center most probe, appears to have the the largest variation away from the average. The deviations away from the average for he central static/total pressure probe indicate that it is being effected by something that causes the measurements to vary from the

average.

We see that the pressure readings from the probes closer to the top of the wind tunnel (T7, T9, S5) appear to be lower (i.e. negative variation) and the probes closer to the bottom of the wind tunnel (T6, T8, S4) appear to be higher (i.e. positive variation). This indicates to us that the pressure is higher in the lower sections of the wind tunnel. We also see that the probes (both static and total) on the left and right support (which is in the vertical center of the test section) do not vary away from the average as much as the vertical probes indicating that the vertical distribution of pressure effects the average more than the horizontal distribution.

3.4 Percentage Difference Between q_{actual} and Omega Transducer/Manometer

In order to investigate the differences between the actual pressure (q_{actual} and the pressures measured by the Omega Transducer (ΔP_{Ω}) and the Manometer ($\Delta P_{measured}$) we need to find the percentage differences between these values. To do so we used the following equations:

$$\text{Percentage Difference Between } q_{actual} \text{ and } \Delta P_{\Omega} = \frac{\Delta P_{\Omega} - q_{actual}}{q_{actual}} * 100[\%] \tag{9}$$

$$\text{Percentage Difference Between } q_{actual} \text{ and } P_{measured} = \frac{P_{measured} - q_{actual}}{q_{actual}} * 100[\%] \tag{10}$$

Computing the percentage differences for each data point we get the following table:

Table 4: Omega Transducer and Manometer Pressure vs Actual Dynamic Pressure

Data Point	**Motor Speed [rpm]**	q_{actual} **[psid]**	ΔP_{Ω} **[psid]**	$q_{actual}/\Delta P_{\Omega}$ **Percentage Difference**	$\Delta P_{measured}$ **[dpsi]**	$q_{actual}/\Delta P_{measured}$ **Percentage Difference**
1	400	4.67E-03	5.64E-03	20.87%	5.42E-03	16.17%
2	500	7.73E-03	9.10E-03	17.79%	9.39E-03	21.52%
3	600	1.14E-02	1.34E-02	17.10%	1.34E-02	17.18%
4	700	1.62E-02	1.89E-02	16.48%	1.88E-02	15.80%
5	800	2.18E-02	2.47E-02	13.49%	2.46E-02	12.76%
6	900	2.73E-02	3.15E-02	15.33%	3.18E-02	16.28%
7	1000	3.40E-02	3.85E-02	13.44%	3.94E-02	15.91%
8	1100	4.24E-02	4.80E-02	13.37%	4.84E-02	14.30%
9	1200	5.19E-02	5.75E-02	10.84%	5.78E-02	11.36%
10	1300	6.00E-02	6.64E-02	10.67%	6.79E-02	13.20%
11	1400	7.06E-02	7.76E-02	9.98%	7.80E-02	10.55%

From Table 7 we see that the percentage difference between q_{actual} and the Omega Transducer/-Manometer readings reduce as the motor speed and velocity increase. These inaccuracies may be due to the Manometer and the Omega Transducer having a sensitivity threshold. Once the velocity and pressure go past a given value the readings become more accurate as the two instruments are able to properly gather the data. Additionally the inaccurate readings may be due to the placement of the instruments within the test section. If they are placed behind or in front the rake the instruments or the pressure probes may encounter non-ideal flow leading to inaccurate measurements.

3.5 Calibration Coefficient

To properly calibrate our wind tunnel for future experiments we have to find a calibration coefficient by graphing q_{actual} against ΔP_{Ω} and taking the slope of the best fit linear line. We graphed this in Figure 7:

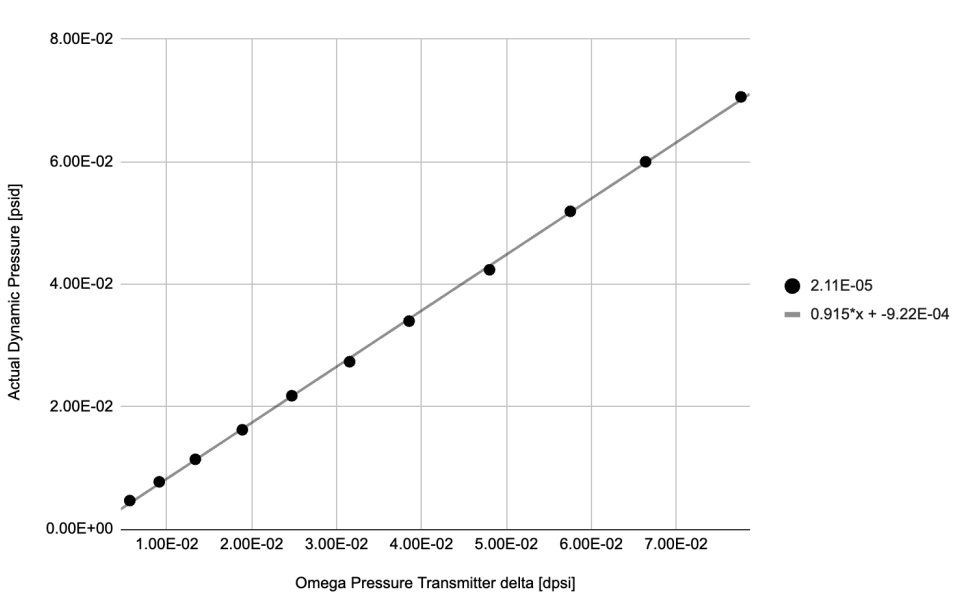

Figure 6: Actual Dynamic Pressure q_{actual} [psid] v.s. Omega Pressure Transmitter delta ΔP_{Ω} [dpsi]

From the equation of the best fit line we see that we get a calibration coefficient of **0.915**. We notice that the trend appears to be linear which we expect as the numbers from both readings should increase linearly as the motor speed increases. While we would expect the calibration coefficient to be 1 in an ideal experiment but the positioning of the Omega Pressure Transducer away from the pressure rake will lead to their readings being slightly different.

The reason for us needing a calibration coefficient is to allow us to get the correct value of $\boldsymbol{q_{actual}}$. This is due to the Omega Pressure Transducer's pressure reading being offset due to the physical properties of the wind tunnel. Using the calibration coefficient we should be able to adjust the readings of the Omega Pressure Transducer to get a more accurate $\boldsymbol{q_{actual}}$ reading from it.

3.6

$$U_{Vactual} = \sqrt{(\frac{\partial V}{\partial p_o}U_{p_o})^2 + (\frac{\partial V}{\partial p_s}U_{p_s})^2 + (\frac{\partial V}{\partial \rho}U_{\rho})^2} \quad (11)$$

where V is the velocity, p_o and p_s are the total and static pressures respectively, and ρ is the density. Therefore, $U_{Vactual}$ is the uncertainty of the actual velocity, and U_{p_o}, U_{p_s}, and U_ρ are the uncertainties of the total pressure, static pressure, and density, respectively. The three partials of velocity with respect to p_o, p_s, and ρ are represented by $\frac{\partial V}{\partial p_o}$, $\frac{\partial V}{\partial p_s}$, and $\frac{\partial V}{\partial \rho}$. After performing the necessary calculations and substitutions (8.1), the following was produced:

Table 5: Uncertainties of the Actual Velocity Values

Data Point	**Motor RPM**	Actual Velocity [ft/s]	Actual Velocity Uncertainty [ft/s]	Uncertainty (%)
1	400	23.17	±8.436E-01	±3.641
2	500	29.82	±1.079	±3.620
3	600	36.23	±1.309	±3.613
4	700	43.20	±1.560	±3.610
5	800	50.07	±1.807	±3.609
6	900	56.09	±2.024	±3.608
7	1000	62.52	±2.256	±3.608
8	1100	69.81	±2.518	±3.607
9	1200	77.28	±2.788	±3.607
10	1300	83.09	±2.997	±3.607
11	1400	90.12	±3.251	±3.607

As shown in the table, as the actual velocity increased, the uncertainty for the actual velocity also increased. This behavior was expected as the errors would be directly proportionate to the values. The percent uncertainty remained relatively constant, demonstrating a fixed trend in the errors relative to the size of the actual velocity values. The source of the highest level of uncertainty, according to the data, was inaccurate calibration for a Motor RPM of 0. Spending slightly more time on the calibration step might have made the uncertainty values lower, but this is partially speculative.

4 CONCLUSIONS

The goal of this lab was to begin to understand the overall characteristics of the wind tunnel and how we need to calibrate it to collect accurate data in future labs. After completing this lab, it is clear that the initial goal of estimating wind tunnel flow characteristics, such as speed and dynamic pressure using various pressure-measurement devices, has been met. By averaging the rake sensor readings at each data point, we were able to determine a corresponding estimated air speed value for the test section with an average uncertainty of ±3.612% across all data points. As expected, the collected data in Figure 3 of Section 3.2 reveals positively associated linear trends in the actual velocity, Reynolds number, and mach number, with respect to increasing motor rotations per minute. The dynamic pressure vs. motor speed graph reveals an exponential relationship and agrees with the equation used to calculate V_{actual}. In section 3.3 we concluded that the variation in pressure along the vertical axis appears to drive the average value as they vary more than the pressure reading along the horizontal axis. It is important to note that percentage differences in Table 4 of Section 3.4 show a decrease as the measured pressure increases. This can be caused by the way the pressure sensors in the rake are designed to function since it reads the deflection of a small plate. It is expected that at lower speeds, the deflection might be much harder to read. Performing this lab has also revealed an important calibration coefficient of 0.915 that will allow us to acquire more accurate data in the future when using the Omega Pressure Transducer to determine q_{actual}. Table 5 in Section 3.6 shows that the actual velocity uncertainty percentage decreases as the motor speed increases highlighting the importance of having a calibration coefficient for our future labs. This means that we can expect more accurate data at high RPMs/flow velocity.

This lab provides room for future improvement, predominantly when it comes to reducing uncertainty. By using the newfound calibration coefficient, we could acquire better data from the Omega Pressure Transducer if the lab were to be repeated. By changing the apparatus to use a rake with more pressure sensors, we would be able to reduce U_p and effectively reduce the overall uncertainty for the estimated actual velocity. By adding more data points in between the collected

ones, we may also extract a more accurate calibration coefficient.

5 REFERENCES

[1] "Wind Tunnel Calibration", Laboratory Writeup for AE 460, University of Illinois at Urbana-Champaign, 2022.

[2] Basic Educational Wind Tunnel Operations Manual, Aerolab, June 2009.

APPENDIX

A Sample Calculations

A.1 P_{0avg} Sample Calculation

The following sample calculation is done for data point 1:

$$P_{0avg} = \frac{1.34E-05 + 4.64E-05 + \ldots + 1.32E-05 + (-1.70E-06)}{9}$$
$$= 4.72E-03 psid$$

A.2 P_{Savg} Sample Calculation

The following sample calculation is done for data point 1:

$$P_{0avg} = \frac{1.85E-05 + (-3.73E-05) + 2.68E-05 + 2.80E-06 + (-1.87E-05)}{5}$$
$$= 5.24E-05 psid$$

A.3 q_{actual} Sample Calculation

The following sample calculation is done for data point 1:

$$q_{actual} = P_{0avg} - P_{Savg}$$
$$= 4.72E-03 - 5.24E-05$$
$$= 4.67E-03$$

A.4 ρ (density) Sample Calculation

The following sample calculation is done using values from data point 1:

$$\begin{aligned}\rho &= \frac{p_{ambient}}{R * T_{ambient}} \\ &= \frac{1.43E+01 * 144}{1716 * 5.33E+02} \\ &= 0.00225 \frac{lb_m}{ft^3}\end{aligned}$$

A.5 V_actual Sample Calculation

The following sample calculation is done using values from data point 1:

$$\begin{aligned}V_{actual} &= \frac{2 * q_{actual} * 144}{\rho} \\ &= \frac{2 * 4.67E-03 * 144}{0.00225} \\ &= 24.42 \frac{ft}{s}\end{aligned}$$

A.6 Reynolds Number Sample Calculation

The following sample calculation is done using values from data point 1:

$$\begin{aligned}\frac{Re}{L} &= \frac{\rho * V_{actual}}{\mu} \\ &= \frac{0.00225 * 24.42}{3.82E-07} \\ &= 144153.74 \frac{1}{ft}\end{aligned}$$

A.7 Mach Number Sample Calculation

The following sample calculation is done using values from data point 1:

$$M = \frac{V_{actual}}{\sqrt{\gamma * R * T_{ambient}}}$$
$$= \frac{24.42}{\sqrt{1.4 * 1716 * 5.33E+02}}$$
$$= 0.022$$

A.8 Total Pressure Variation Sample Calculation

The following sample calculation is for Rake T1 at data point 1:

$$TPV_{(1,1)} = \frac{P_{0,1} - P_{0avg}}{q_{actual}} * 100[\%]$$
$$= \frac{4.75E-03 - 4.72E-03}{4.67E-03} * 100[\%]$$
$$= 0.69\%$$

A.9 Static Pressure Variation Sample Calculation

The following sample calculation is for Rake S1 at data point 1:

$$TPV_{(1,1)} = \frac{P_{S,1} - P_{Savg}}{q_{actual}} * 100[\%]$$
$$= \frac{5.27E-05 - 5.24E-05}{4.67E-03} * 100[\%]$$
$$= 0.00\%$$

A.10 Percentage Difference Calculation

The following sample calculation is conducted for the percentage difference between q_{actual} and ΔP_{Ω} for data point 1 but the same method can be applied for all other percentage difference

calculations in this lab:

$$\text{Percentage Difference Between } q_{actual} \text{ and } \Delta P_{\Omega} = \frac{\Delta P_{\Omega} - q_{actual}}{q_{actual}} * 100$$
$$= \frac{5.64E-03 - 4.67E-03}{4.67E-03} * 100$$
$$= 20.87\%$$

A.11 Derivation/Calculation of Actual Velocity Uncertainty

$$U_{Vactual} = \sqrt{(\frac{\partial V}{\partial p_o} U_{p_o})^2 + (\frac{\partial V}{\partial p_s} U_{p_s})^2 + (\frac{\partial V}{\partial \rho} U_{\rho})^2} \tag{12}$$

V was given by the following formula:

$$V = \sqrt{\frac{2(P_o - P_s)}{\rho}} \tag{13}$$

For the motor speed of 1000 RPM, the values of P_{amb} and T_{amb} were 1.43E+01 Psia and 5.33E+02 R respectively.

$$\rho = \frac{P_{amb}}{RT_{amb}} = \frac{\text{1.43E+01 Psia}}{10.73 * \text{5.33E+02 R}} = \text{2.50E-03} \tag{14}$$

and

$$p_o - p_s = \text{3.40E-02} \tag{15}$$

The three partials were calculated through a derivative calculator. Then the mentioned values shown above were substituted as follows:

$$\frac{\partial V}{\partial p_o} = \sqrt{\frac{1}{2\rho(p_o - p_s)}} = \sqrt{\frac{1}{2(\text{2.50E-03})(\text{3.40E-02})}} = \text{7.668E+01} \tag{16}$$

$$\frac{\partial V}{\partial p_s} = -\sqrt{\frac{1}{2\rho(p_o - p_s)}} = -\sqrt{\frac{1}{2(\text{2.50E-03})(\text{3.40E-02})}} = -\text{7.668E+01} \tag{17}$$

$$\frac{\partial V}{\partial \rho} = -\sqrt{\frac{(p_o - p_s)}{2\rho^3}} = -\sqrt{\frac{(3.40\text{E-}02)}{2(2.50\text{E-}03)^3}} = \text{-}1.041\text{E+}03 \tag{18}$$

To find the uncertainty of ρ,

$$U_\rho = \sqrt{(\frac{\partial \rho}{\partial P_{amb}} U_{P_{amb}})^2 + (\frac{\partial \rho}{\partial R} U_R)^2 + (\frac{\partial \rho}{\partial T_{amb}} U_{T_{amb}})^2} \tag{19}$$

The uncertainties of P_{amb} and T_{amb} were ±0.0727 Psia and ±461.47 R, respectively. The partials were calculated as follows:

$$\frac{\partial \rho}{\partial P_{amb}} = \frac{1}{RT_{amb}} = \frac{1}{10.73 * 5.33\text{E+}02\ \text{R}} = 1.75\text{E-}04 \tag{20}$$

$$\frac{\partial \rho}{\partial R} = 0 \tag{21}$$

$$\frac{\partial \rho}{\partial T_{amb}} = -\frac{P_{amb}}{RT_{amb}^2} = -\frac{1.43\text{E+}01\ \text{Psia}}{R(5.33\text{E+}02\ \text{R})^2} = \text{-}4.70\text{E-}06 \tag{22}$$

Therefore,

$$U_\rho = \sqrt{(1.75\text{E-}04 * \pm 0.0727\ \text{Psia})^2 + (0)^2 + (\text{-}4.70\text{E-}06 * \pm 461.47\ \text{R})^2} = \pm 2.167\text{E-}03 \tag{23}$$

To find U_{p_o} and U_{p_s},

$$U_p = \sqrt{(\frac{1}{n} U_{p1})^2 + (\frac{1}{n} U_{p2})^2 + (\frac{1}{n} U_{p3})^2 + \ldots + (\frac{1}{n} U_{pn})^2} \tag{24}$$

The uncertainties for the pressures measured here were ±0.1% of 1 psi, which simplified to ±0.001 psi. Therefore,

$$U_{p_s} = \sqrt{5 * (\frac{1}{5} * (\pm 0.001\ \text{psi}))^2} = \pm 4.472\text{E-}04\ \text{psi} \tag{25}$$

$$U_{p_o} = \sqrt{9 * (\frac{1}{9} * (\pm 0.001\ \text{psi}))^2} = \pm 3.333\text{E-}04\ \text{psi} \tag{26}$$

All of the values were substituted into equation (10) to find the uncertainty of the actual velocity:

$$\boldsymbol{U_{Vactual}} = \sqrt{(7.668\text{E+}01 * 3.333\text{E-}04)^2 + (-7.668\text{E+}01 * 4.472\text{E-}04)^2 + (-1.041\text{E+}03 * 2.167\text{E-}03)^2}$$
$$= \pm 2.255 \frac{\text{ft}}{\text{s}} \tag{27}$$

The percent uncertainty was calculated as follows:

$$\%\text{ uncertainty} = \frac{\mathbf{100} * \boldsymbol{U_{Vactual}}}{\boldsymbol{Vactual}} \% = \frac{\mathbf{100} * (\pm 2.255 \frac{\text{ft}}{\text{s}})}{62.52 \frac{\text{ft}}{\text{s}}} \% = \mathbf{3.608}\ \%\text{ uncertainty} \tag{28}$$

B Raw Data

Data Table for Wind Tunnel Calibration Experiment

Name: Praneesh Kumar

Section/Group: ABT Date: 8/31/2022

Ambient conditions:
Pressure ("Hg): 29.15

Temperature (°F): 73.4

Residual zero-velocity ΔP_Ω offset from the Omega transmitter: 5.94 E-6 (dpsi)

Data Point	Motor Speed (RPM)	$\Delta P_{Measured}$ Dwyer (" W.C.)	ΔP_Ω Omega trans. (dpsi)	Average Rake q (dpsi)	Average Rake Velocity (ft/s)
1	400	0.00542	0.00564	0.00467	24.415
2	500	0.00939	0.00910	0.00773	31.428
3	600	0.01337	0.01336	0.01141	38.1797
4	700	0.018786	0.018896	0.01622	45.5311
5	800	0.024567	0.02472	0.02179	52.7635
6	900	0.03179	0.03153	0.02734	59.1089
7	1000	0.03937	0.03854	0.03397	65.8893
8	1100	0.04841	0.04802	0.04235	73.5689
9	1200	0.05780	0.05753	0.05191	81.4438
10	1300	0.06792	0.06640	0.05999	87.5614
11	1400	0.07806	0.07764	0.07059	94.976
12					
13					
14					
15					
16					

Figure 7: Lab 1 Raw Data

C GROUP MEMBER CONTRIBUTIONS

Group Member	Contribution to Laboratory Note for Experiment 3
Blizhaid Estrada	Conclusion (4)
Shyam Thyagarajan	Data Analysis (3.6), Sample Calculations (A.11)
Dylan D'Silva	Introduction (1), Apparatus (2)
Prahersh Kumar	Data Analysis (3.1-3.5), Sample Calculations (A.1-A.10), References (6)